

AKARI Near-Infrared Spectroscopy of Galactic H II regions

Tamami I. Mori^{a*}, Takashi Onaka^a, Itsuki Sakon^a, Daisuke Ishihara^b, Takashi Shimonishi^c, Ryou Ohsawa^a and Aaron C. Bell^a

^a*Department of Astronomy, Graduate School of Science, The University of Tokyo, Tokyo 113-0033, Japan*

^b*Graduate School of Science, Nagoya University, Nagoya 464-8602, Japan*

^c*Department of Earth and Planetary Sciences, Faculty of Science, Kobe University, 1-1 Rokkodai-cho, Nada Kobe 657-8501 Japan*

E-mail: morii@astron.s.u-tokyo.ac.jp

We performed 2.5–5.5 μm near-infrared slit-spectroscopic observations for 36 Galactic H II regions with the infrared camera onboard the *AKARI* satellite. In addition to the well-known 3.3–3.6 μm features, a relatively weak emission feature is detected at around 5.0–5.4 μm with sufficient signal-to-noise ratios, which we identify as the previously reported PAH 5.25 μm band. The band correlates well with both the aromatic 3.3 μm feature and the aliphatic 3.4–3.6 μm features, which supports that the 5.25 μm band comes from C-H vibration modes of PAHs. The analysis also shows the systematic variation of the ratio of $I(3.4\text{--}3.5)/I(3.3)$ against the ratio of $I(3.7, \text{cont})/I(3.3)$ and the decrease of the *AKARI* mid-infrared color of 9 μm to 18 μm with the transition from photodissociation region (PDR)-dominated to ionized gas-dominated regions. These facts may possibly reflect some dust processing inside the ionized-gas or its boundary.

*The Life Cycle of Dust in the Universe: Observations, Theory, and Laboratory Experiments - LCDU 2013, 18-22 November 2013
Taipei, Taiwan*

*Speaker.

The wavelength range of 2–5 μm includes a number of emission and/or absorption features related to various kinds of materials in the interstellar medium (ISM). However, in spite of its observational significance, this wavelength range has not drawn much attention so far. The Japanese infrared satellite *AKARI* [4] has higher sensitivity than ever before at near-infrared (NIR) wavelengths. Since the advent of *AKARI*, the richness and the importance of this wavelength range has been gradually recognized.

1. Observations and Results

We now introduce our current work on NIR slit-spectroscopy of Galactic H II regions with the infrared camera [5] onboard *AKARI*. The observations were done for 36 Galactic H II regions as a part of a director's time program. For the purpose of the calibration, grism and prism spectroscopy (2.5–5.0 μm , $R \sim 100$ for the grism and 1.7–5.4 μm , $R \sim 20$ –40 for the prism) were done for the same slit area ($\sim 1' \times 0.5''$) in the first and the latter half of a single pointing observation separately.

As shown in Fig.1, the spectra are abundant in ISM features. Major components are as follows: hydrogen recombination lines (e.g. Br β at 2.63 μm , Br α at 4.05 μm , and Pf β at 4.65 μm), the PAH 3.3 μm band and its weak satellite-features at around 3.4–3.6 μm . In addition to them, an emission band appears at around 5.0–5.4 μm , which we identify as the PAH 5.25 μm band.

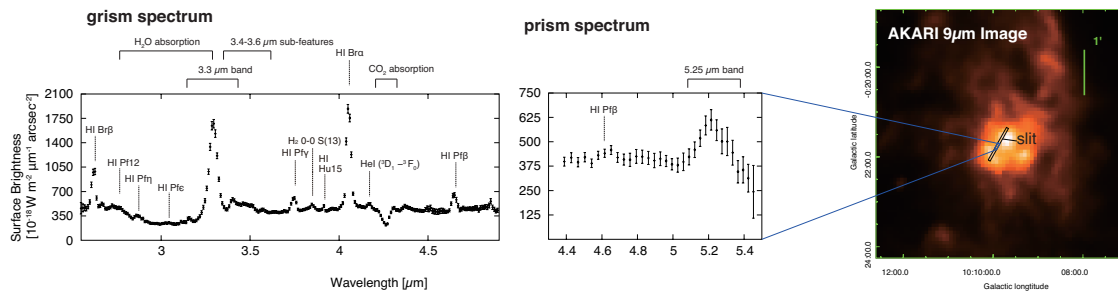


Figure 1: A typical example of the spectra obtained by the present observations and the *AKARI* 9 μm image of the target source. On the S9 image, the spectra-extracted region is indicated by a blue box. We extract a grism and a prism spectrum from the same area with the length of 6 pixels ($\sim 9''$) along the slit, which is indicated by a black box.

1.1 Detection of the 5.25 μm band

Several studies have suggested that the 5.25 μm band comes from combination, difference, and overtone bands of C-H vibration modes of PAHs [1]. However, due to its relatively weak emission and the position at the edges of coverage of IR detectors, only a few observational reports are available on the 5.25 μm band so far. In this study, thanks to *AKARI*'s high sensitivity, we can detect the 5.25 μm with sufficient signal-to-noise ratios in most resultant spectra. Fig.2 shows that the 5.25 μm band correlates well with the 3.3 μm band and the 3.4–3.6 μm sub-features, both of which are associated with C-H vibration modes. The present results strongly support previous studies and also suggest that the 5.25 μm band is useful for probing PAH size distribution as an alternative to the 3.3 μm band [3].

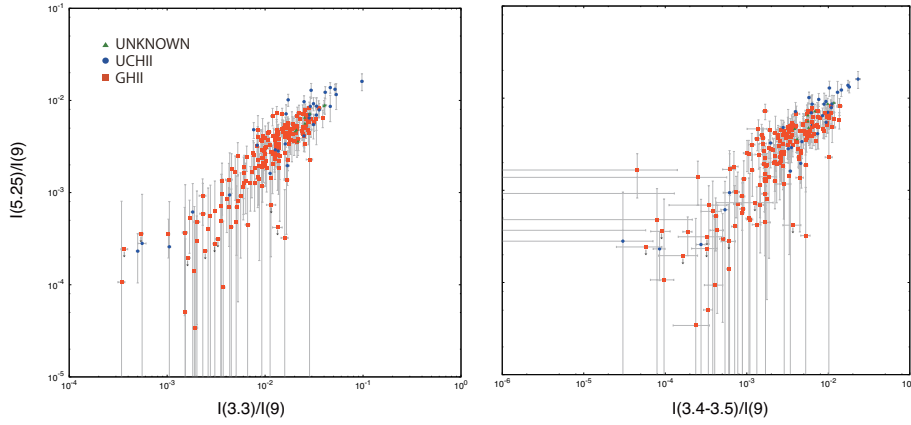


Figure 2: Plots of the ratio of the 5.25 μm band to the AKARI 9 μm surface brightness versus that of the 3.3 μm band (*Left*) and the 3.4–3.6 μm sub-features (*Right*). The downward arrows indicate upper limits, where the 5.25 μm band is not detected. The upper limits are calculated from the spectral uncertainty.

1.2 An aliphatic-to-aromatic ratio of $I(3.4-3.5)/I(3.3)$

The PAH 3.3 μm band is commonly accompanied by weak satellite-features at around 3.4–3.6 μm . These satellite-features are thought to originate in vibration modes of aliphatic C-H bonds. Thus, the relative intensity of the 3.4–3.6 μm features to the 3.3 μm band, which is assigned to aromatic C-H vibration modes, can tell us the aromatic-aliphatic nature of astronomical PAHs. The ratio of $I(3.4-3.5)/I(3.3)$ decreases, as the ratio of the 3.7 μm continuum emission to the 3.3 μm band increases (see Fig.3). The ratio of $I(3.7, \text{cont})/I(3.3)$ mirrors the PAH ionization degree [2]. Assuming that the density and temperature of the gas do not vary significantly, $I(3.7, \text{cont})/I(3.3)$ traces the intensity of the UV radiation field. Aliphatic C-H bonds are less resilient than aromatic ones and require less energy to break. The observed trend can be interpreted as aliphatic C-H bonds being efficiently destroyed prior to aromatic ones with the evolution of the UV radiation field.

1.3 MIR color of 9 to 18

The analysis also shows that the MIR color of $I(9)/I(18)$ obtained from the AKARI MIR all-sky survey steeply declines against the ratio of the hydrogen recombination line $\text{Br}\alpha$ to the 3.3 μm band. The ratio of $I(\text{Br}\alpha)/I(3.3)$ indicates the fraction of the ionized gas along the line of sight. The present result suggests that the 18 μm emission becomes stronger relative to the 9 μm emission with the transition from PDR-dominated to ionized gas-dominated regions. This can be explained by PAH destruction and either very small grain (VSG) or big grain (BG) replenishment inside the ionized gas, which are proposed by several authors as a possible interpretation of *Herschel* and *Spitzer* multiwavelength observations [6]. However, the origin of the 18 μm emission is still unclear, and we cannot draw a clear conclusion at the moment.

Some spectra also show clear absorption features due to H_2O , CO_2 , and CO ices. Furthermore,

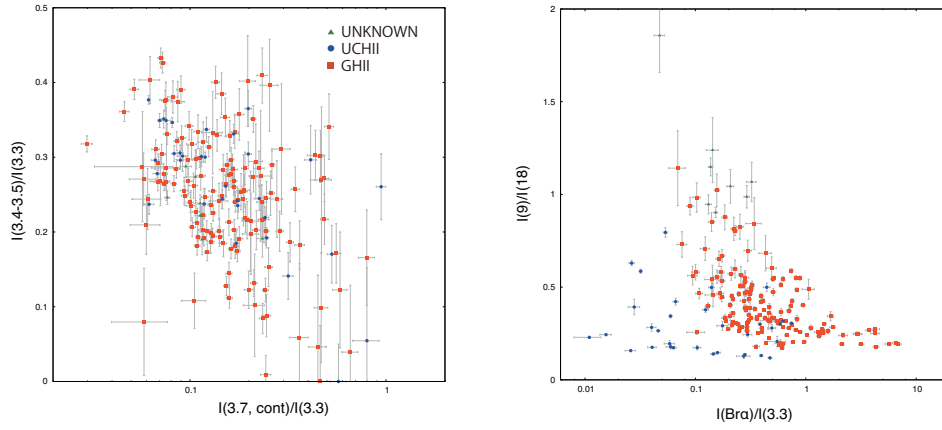


Figure 3: Plots of the ratio of $I(3.4-3.5)/I(3.3)$ versus $I(3.7, cont)/I(3.3)$ (Left) and of $I(9)/I(18)$ versus $I(Br\alpha)/I(3.3)$ (Right).

we detect a XCN absorption feature at $4.67 \mu\text{m}$ in two objects including Sgr A. Detailed analysis and discussion will be reported separately.

Acknowledgement

This work is based on observations with *AKARI*, a JAXA project with the participation of ESA. We thank all the members of the *AKARI* project for their continuing support and encouragement. This work is supported in part by Grants-in-Aid for Scientific Research from the Japan Society of Promotion of Science (JSPS). T. I. M. and R. O. receive financial support from a Grant-in-Aid for JSPS Fellows.

References

- [1] Boersma, C., Mattioda, A. L., Bauschlicher, Jr., C. W., et al. 2009, *ApJ*, 690, 1208
- [2] Haraguchi, K., Nagayama, T., Kurita, M., Kino, M., & Sato, S. 2012, *PASJ*, 64, 127
- [3] Mori, T. I., Sakon, I., Onaka, T., et al. 2012, *ApJ*, 744, 68
- [4] Murakami, H., Baba, H., Barthel, P., et al. 2007, *PASJ*, 59, 369
- [5] Onaka, T., Matsuhara, H., Wada, T., et al. 2007, *PASJ*, 59, 401
- [6] Paladini, R., Umana, G., Veneziani, M., et al. 2012, *ApJ*, 760, 149